J. Fluid Mech. (1994), *vol.* 281, *pp.* 119–135

Transitional flow between contra-rotating disks

By M. KILIC†, X. GAN AND J. M. OWEN
School of Mechanical Engineering, University of Bath, Claverton Down, Bath, BA2 7AY, UK

(Received 15 November 1993 and in revised form 30 June 1994)

This paper describes a combined computational and experimental study of the flow between contra-rotating disks for $-1 \leqslant \Gamma \leqslant 0$ and $Re_\phi = 10^5$, where Γ is the ratio of the speed of the slower disk to that of the faster one and Re_ϕ is the rotational Reynolds number of the faster disk. For $\Gamma = 0$, the rotor-stator case, laminar and turbulent computations and experimental measurements show that laminar Batchelor-type flow occurs: there is radial outflow in a boundary layer on the rotating disk, inflow on the stationary disk and a rotating core of fluid between. For $\Gamma = -1$, the laminar computations produce Batchelor-type flow: there is radial outflow on both disks and inflow in a free shear layer in the mid-plane, on either side of which is a rotating core of fluid. The turbulent computations and the velocity measurements for $\Gamma = -1$ show Stewartson-type flow: radial outflow occurs in laminar boundary layers on the disks and inflow occurs in a non-rotating turbulent core between the boundary layers. For intermediate values of Γ, transition from Batchelor-type flow to Stewartson-type flow is associated with a two-cell structure, the two-cells being separated by a streamline that stagnates on the slower disk; Batchelor-type flow occurs radially outward of the stagnation point and Stewartson-type flow radially inward. The turbulent computations are mainly in good agreement with the measured velocities for $\Gamma = 0$ and $\Gamma = -1$, where either Batchelor-type flow or Stewartson-type flow occurs; there is less good agreement at intermediate values of Γ, particularly for $\Gamma = -0.4$ where the double transition of Batchelor-type flow to Stewartson-type flow and laminar to turbulent flow occurs in the two-cell structure.

1. Introduction

Contra-rotating turbines may be used in future generations of gas-turbine aero-engines to drive the contra-rotating fans. The flow and heat transfer between the contra-rotating disks, to which the turbine blades are attached, are of interest to the gas-turbine designer, and there is comparatively little information on such flows.

Batchelor (1951) considered the solution of the Navier–Stokes equations for the case of infinite disks in the range $-1 \leqslant \Gamma \leqslant 0$, where Γ is the ratio of the angular speed of the slower disk, Ω_2, to that of the faster one, Ω_1. Assuming similarity solutions, like those used by von Karman (1921), Batchelor produced ordinary differential equations from which he deduced, using physical arguments, the behaviour of the streamlines.

Figures 1(*a*) and 1(*b*) show the streamlines and distributions of the tangential component of velocity, V_ϕ, obtained by Batchelor for $\Gamma = 0$ and $\Gamma = -1$ at large rotational speeds (or, more correctly, at large values of $\Omega_1 s^2/\nu$, where s is the axial spacing and ν the kinematic viscosity). For $\Gamma = 0$, which will be referred to as the rotor-stator case, there is radial outflow in a thin boundary layer on the rotating disk and

† Present address: Uludağ Universitesi, Mühendislik-Mimarlik Fakultesi, Makina Bolumu, Bursa, Turkey.

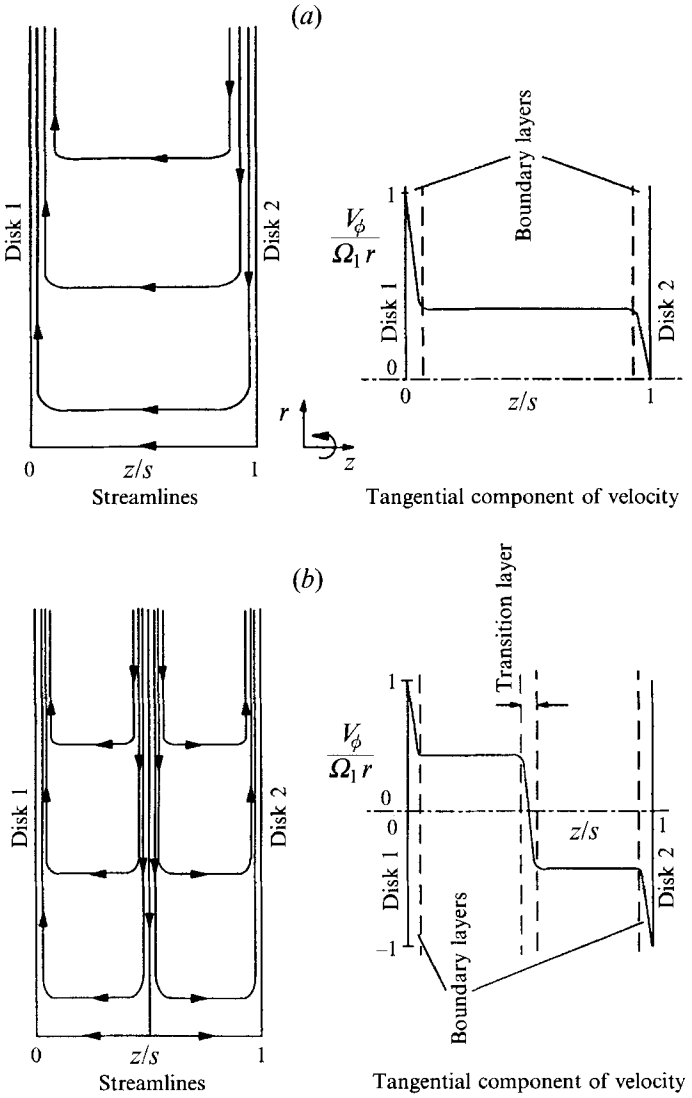

FIGURE 1. Streamlines predicted by Batchelor (1951): (*a*) $\Gamma = 0$; (*b*) $\Gamma = -1$.

inflow on the stationary one. Between the boundary layers, there is a rotating core of fluid in which the radial component of velocity is zero and there is an axial flow from the stationary to the rotating disk. For $\Gamma = -1$, there is radial outflow in the boundary layers on both disks and radial inflow in a free shear layer (termed a transition layer by Batchelor) in the mid-plane ($z/s = \frac{1}{2}$, where z is the axial distance from disk 1). Between the shear layer and each boundary layer is a rotating core of fluid in which the radial component of velocity is zero and there is an axial flow from the shear layer to the adjacent disk. Batchelor noted that, 'This singular solution may not be realizable experimentally, of course, but it has some intrinsic interest.'

Stewartson (1953) obtained series solutions of the Navier–Stokes equations for low Reynolds numbers ($\Omega_1 s^2/\nu \leqslant 40$) and concluded that, for $\Gamma = 0$, there was a boundary layer on the rotating disk but none on the stationary one: there was no evidence of the core rotation predicted by Batchelor. For $\Gamma = -1$, Stewartson showed that there would be radial outflow on both disks, but there was no suggestion of contra-rotating

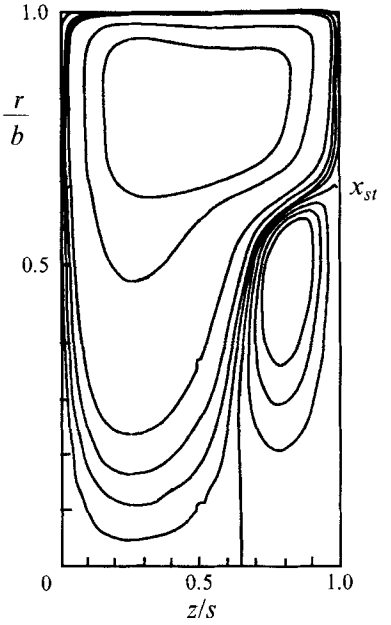

FIGURE 2. Computed streamlines for $\Gamma = -0.3$, $Re_\phi = 2.04 \times 10^4$, $G = 0.07$ (Dijkstra & van Heijst 1983).

cores of fluid. He also carried out rudimentary experiments with two cardboard disks of 150 mm diameter, spaced up to 125 mm apart, and found no signs of core rotation for $\Gamma = 0$ or $\Gamma = -1$.

The Batchelor–Stewartson controversy has been the subject of many studies, and the interested reader is referred to Zandbergen & Dijkstra (1987) for a detailed description. For infinite disks, there are multiple solutions of the equations, of which Batchelor's and Stewartson's are both possible. For finite disks, however, the solution depends on whether the disks are open or enclosed: an enclosed rotor-stator system ($\Gamma = 0$) tends to produce Batchelor-type flow with core rotation; disks open to the atmosphere tend to produce Stewartson-type flow with no core rotation.

A comprehensive computational and experimental study of laminar flow between contra-rotating disks was conducted by Dijkstra & van Heijst (1983) for $-0.825 \leqslant \Gamma \leqslant 0$. Experimental measurements were made in a rig with glass disks of around 1 m diameter separated by a gap of 35 mm ($G = 0.07$, where $G = s/b$, b being the radius of the disks), and the fluid was water or a mixture of water and glycerine. For $\Gamma = 0$, they found Batchelor-type flow with radial outflow on the rotating disk, inflow on the stationary one, and a rotating core of fluid between. For $-0.825 \leqslant \Gamma \leqslant -0.15$, a two-cell structure was computed and observed, and an example of the computed streamlines for $\Gamma = -0.3$ and $Re_\phi = 2.04 \times 10^4$ (where $Re_\phi = \Omega_1 b^2/\nu$) is shown in figure 2. Circulation is clockwise near the faster disk (the left-hand disk in figure 2) and anticlockwise near the slower one; a streamline separating the two cells stagnates on the slower disk at a non-dimensional radius of $x = x_{st}$ (where $x = r/b$). The value of x_{st} increased as Γ was reduced but no reliable experimental or computational results were obtained for $-1 < \Gamma < -0.825$, where wavy instabilities were observed.

Gan, Kilic & Owen (1993) conducted a combined computational and experimental study for the case of antisymmetrical contra-rotation, $\Gamma = -1$, for $2.3 \times 10^5 \leqslant Re_\phi \leqslant 1.2 \times 10^6$, with and without superposed flow. The experimental apparatus and the

computational method were basically the same as those described below with the exception that a variant of Morse's (1988, 1991*a*, *b*) low-Reynolds-number k–ϵ turbulence model was used in the computations rather than the Launder & Sharma (1974) turbulence model used here. Laminar computations produced the Batchelor-type flow described above; computations using the turbulence model produced only Stewartson-type flow. Laser Doppler anemometry (LDA) measurements confirmed the turbulent computations, and no experimental evidence of Batchelor-type flow was found even for local rotational Reynolds numbers as low as $x^2 Re_\phi = 2.2 \times 10^4$: laminar boundary layers formed on the disks but the radial inflow in the (virtually non-rotating) core was always turbulent.

The purpose of this paper is to study the flow between contra-rotating disks in the range $-1 \leqslant \Gamma \leqslant 0$, and to examine how the transition from Batchelor-type flow at $\Gamma = 0$ to Stewartson-type flow at $\Gamma = -1$ occurs. The computational method is outlined in §2, the experimental apparatus in §3, and a comparison between the computed and measured velocity distributions is presented in §4.

2. Computed flow

2.1. *Computational method*

The Reynolds-averaged axisymmetric steady-state incompressible Navier–Stokes equations, in cylindrical-polar coordinates, were solved using the finite-volume multigrid elliptic solver described by Gan *et al.* (1993). The code used was a modified version of the elliptic multigrid solver described by Vaughan, Gilham & Chew (1989), where finite-volume equations were obtained using the control-volume approach of Patankar (1980) together with the SIMPLEC pressure-correction algorithm proposed by van Doormaal & Raithby (1984). The multigrid method was developed by Vaughan *et al.* for turbulent flow from the full-approximation-scheme employed by Lonsdale (1988) to solve the Navier–Stokes equations for laminar flow between corotating disks; a three-level V-cycle was used for the computations discussed below. Further details of the solver, the turbulence models and the convergence criteria are given by Kilic (1993). For the computations presented in this paper, either the flow was assumed to be laminar or the low-Re k–ϵ turbulence model of Launder & Sharma (1974) was used.

The computational geometry was based on the experimental rig described in §3 (and shown in figure 7). At the outer radius of the rig, $r = b$, a cylindrical 'shroud' was attached to each disk, and at the inner radius, $r = a$, a cylindrical tube was attached to each disk. There was a small axial clearance, s_c, between the contra-rotating shrouds and between the contra-rotating tubes, and an axial clearance, s, between the disks. The geometry was defined in non-dimensional terms by: $G = s/b = 0.12$, $G_c = s_c/b = 0.016$ and $a/b = 0.13$.

No-slip boundary conditions were used for all solid surfaces: V_r and V_z were set to zero, and V_ϕ was set to the appropriate speed of rotation. For the clearance between the shrouds at $r = b$ and between the tubes at $r = a$, V_r and V_z were set to zero, and V_ϕ varied linearly from $\Omega_1 b$ to $\Omega_2 b$ or from $\Omega_1 a$ to $\Omega_2 a$.

Grid-dependency tests were conducted for a number of non-uniform grids with up to 91×115 (axial $\times$ radial) nodes, and a grid with 67×67 nodes was found to give sensibly grid-independent results. The computations were carried out on one of the i860 nodes of a 16-node Meiko parallel computing facility. Typical times to achieve a converged solution on a 91×115 grid, which was used for the results presented below, ranged from 15 minutes to one hour for laminar flow and from one to two hours for turbulent flow.

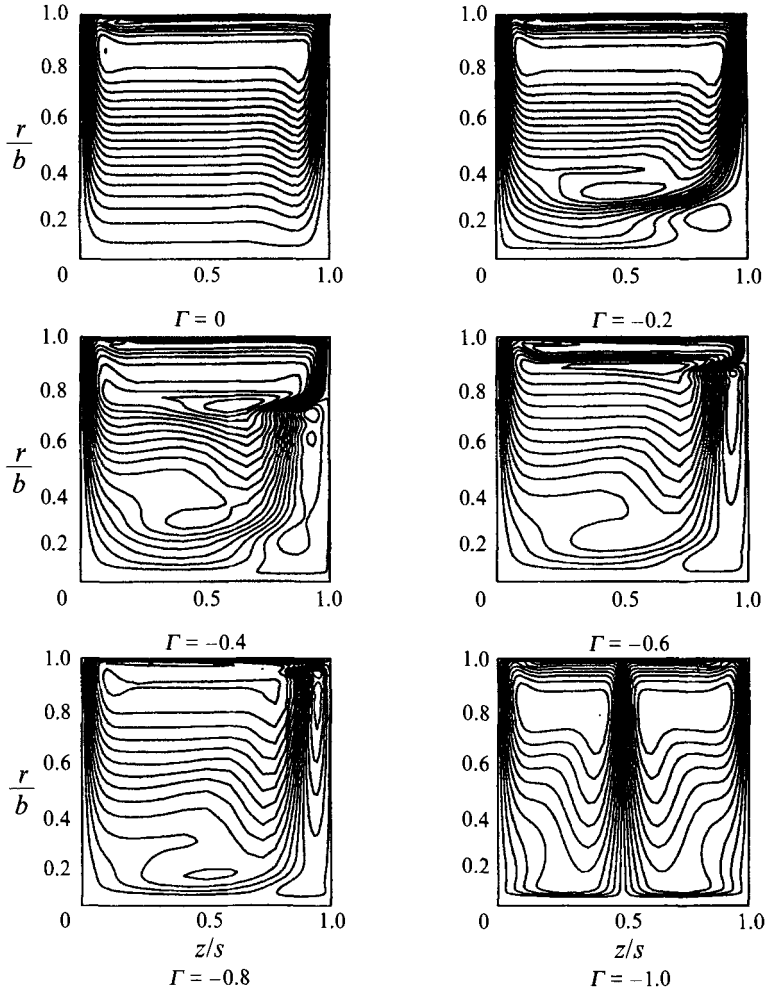

FIGURE 3. Computed laminar streamlines for $Re_\phi = 10^5$, $G = 0.12$.

2.2. *Computed flow structure*

Figure 3 shows the computed streamlines, in the (r, z)-plane, for laminar flow at $Re_\phi = 10^5$. The computations were carried out for $G = 0.12$ but the aspect ratio of the figures has been distorted to clarify the flow structure. The left-hand boundary corresponds to disk 1, the faster disk.

For $\Gamma = 0$, Batchelor-type rotor-stator flow can be seen, with radial outflow in a thin boundary layer on the rotating disk and radial inflow on the stationary one. For $x \leqslant 0.9$, there is an axial flow from the boundary layer on the stationary disk to that on the rotating one. For $x \geqslant 0.9$, the axial flow is in the reverse direction; most of the fluid is transferred axially in a thin boundary layer on the cylindrical shrouds at $x = 1$, but some fluid separates from the boundary layer on the rotating shroud and flows in an axial stream into the boundary layer on the stationary disk.

For $-1 \leqslant \Gamma \leqslant -0.2$, the two-cell structure can be seen, with clockwise circulation near the faster disk and anticlockwise circulation near the slower one. As found by Dijkstra & van Heijst, the stagnation point of the separation streamlines moves radially outward on the slower disk as Γ is reduced. For $-0.8 \leqslant \Gamma \leqslant -0.4$, radial

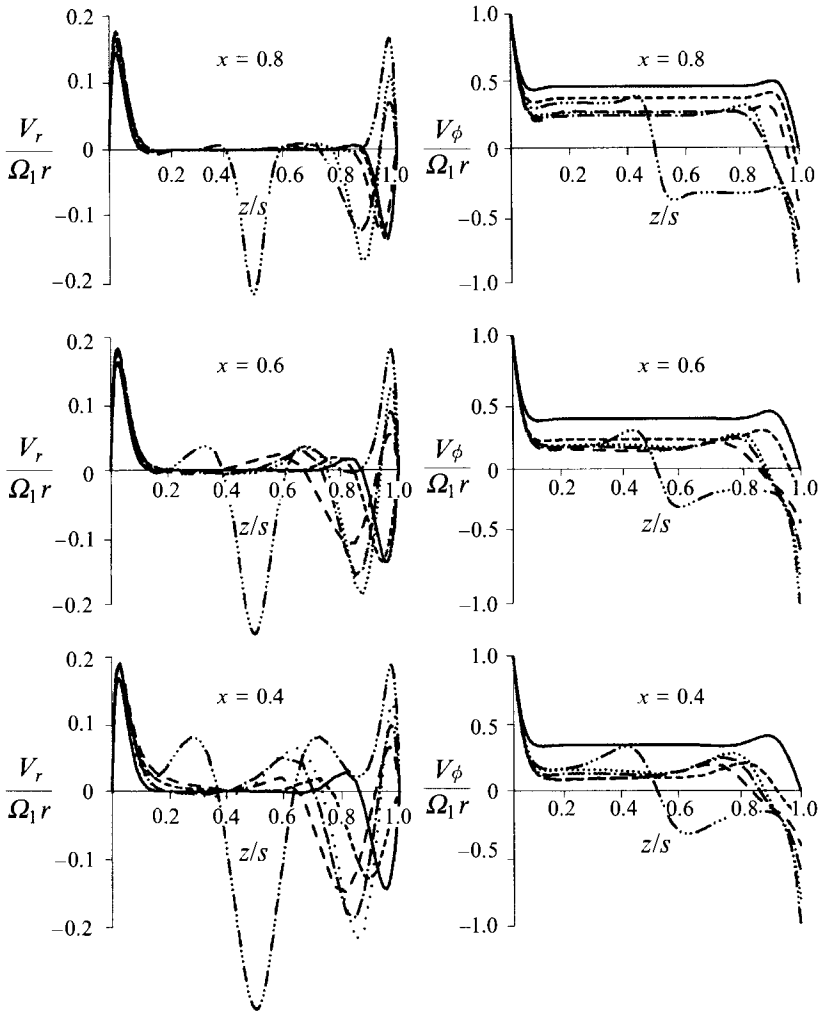

FIGURE 4. Computed laminar velocity distributions for $Re_\phi = 10^5$, $G = 0.12$. ——, $\Gamma = 0$; ---, -0.2; – – –, -0.4; – · –, -0.6; · · · · · ·, -0.8; – · · · –, -1.0.

inflow occurs in a free shear layer that originates near the stagnation point on the slower disk; radially outward of this stagnation point, there is a region of axial flow from the rotating disk to the stationary one. As Γ is reduced, the stagnation point moves radially outward compressing the region of axial flow: for $\Gamma = -0.6$, the region is reduced to a thin free shear layer at $x \approx 0.9$ and a boundary layer on the shroud; for $\Gamma = -0.8$, all the axial flow is confined to the boundary layer. For $\Gamma = -1$, the streamlines are symmetrical about the mid-plane ($z/s = \frac{1}{2}$), and radial inflow occurs in a thin free shear layer in the mid-plane ($z/s = \frac{1}{2}$), consistent with Batchelor-type flow.

The computed distributions of the non-dimensional radial and tangential components of velocity ($V_r/\Omega_1 r$ and $V_\phi/\Omega_1 r$) with the non-dimensional axial distance (z/s), are shown in figure 4. Referring to the distributions for $x = 0.8$, the following observations can be made.

(i) For $-0.4 \leqslant \Gamma \leqslant 0$, there are separate boundary layers on both disks with radial outflow on disk 1 and inflow on disk 2. In the core between the boundary layers, V_r is zero and V_ϕ is invariant with z.

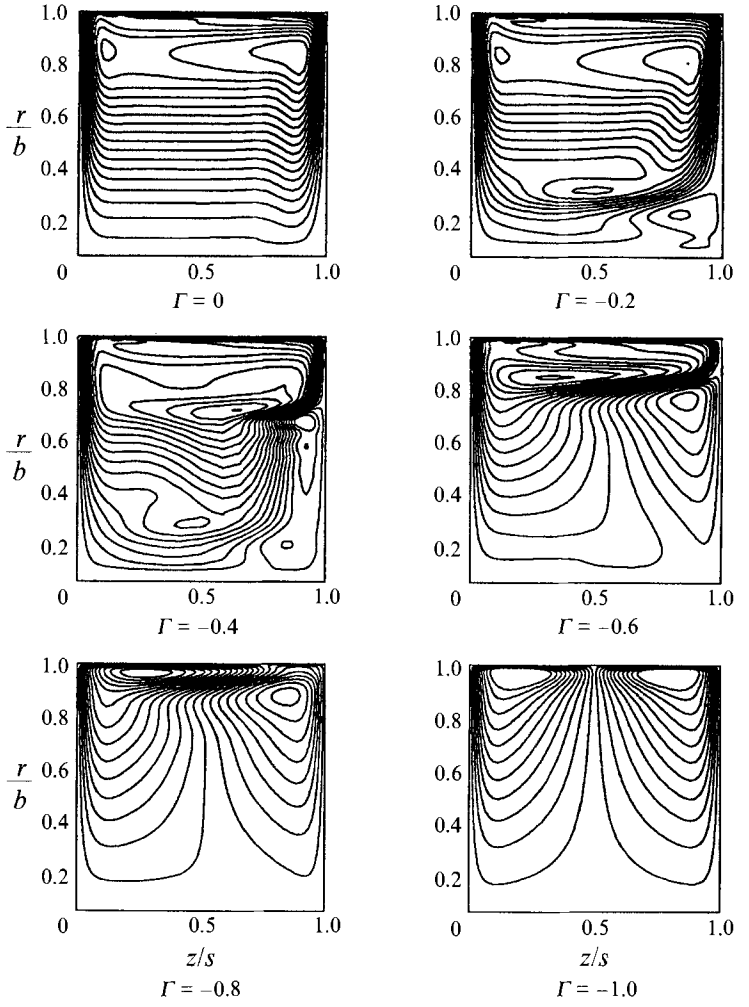

FIGURE 5. Computed turbulent streamlines for $Re_\phi = 10^5$, $G = 0.12$.

(ii) For $-1 \leqslant \Gamma \leqslant -0.6$, there is radial outflow in the boundary layers on both disks, and inflow occurs in a free shear layer close to the slower disk or, for $\Gamma = -1$, in the mid-plane. Also, for $\Gamma = -1$, contra-rotating cores of fluid are formed.

These observations for $x = 0.8$, and the results for $x = 0.4$ and 0.6, are consistent with Batchelor-type flow.

Figures 5 and 6 show the equivalent computations for the case where the turbulence model is used. For $-0.4 \leqslant \Gamma \leqslant 0$, the computed streamlines in figure 5 are broadly similar to those in figure 3 whereas those for $-1 \leqslant \Gamma \leqslant -0.6$ show that, for the turbulent computations, the radial inflow is not confined to a thin free shear layer. Referring to the computed velocity distributions for $x = 0.8$ in figure 6 it can be seen that for $-1 \leqslant \Gamma \leqslant -0.6$ there is very little core rotation and radial inflow occurs over the entire region between the two boundary layers. In particular, the contra-rotating cores have disappeared for $\Gamma = -1$. It appears that, for $-1 \leqslant \Gamma \leqslant -0.6$, transition from laminar to turbulent flow in the core has destroyed the Batchelor-type flow and created Stewartson-type flow. For all the turbulent computations, the flow in the boundary layer on the faster disk always remains laminar.

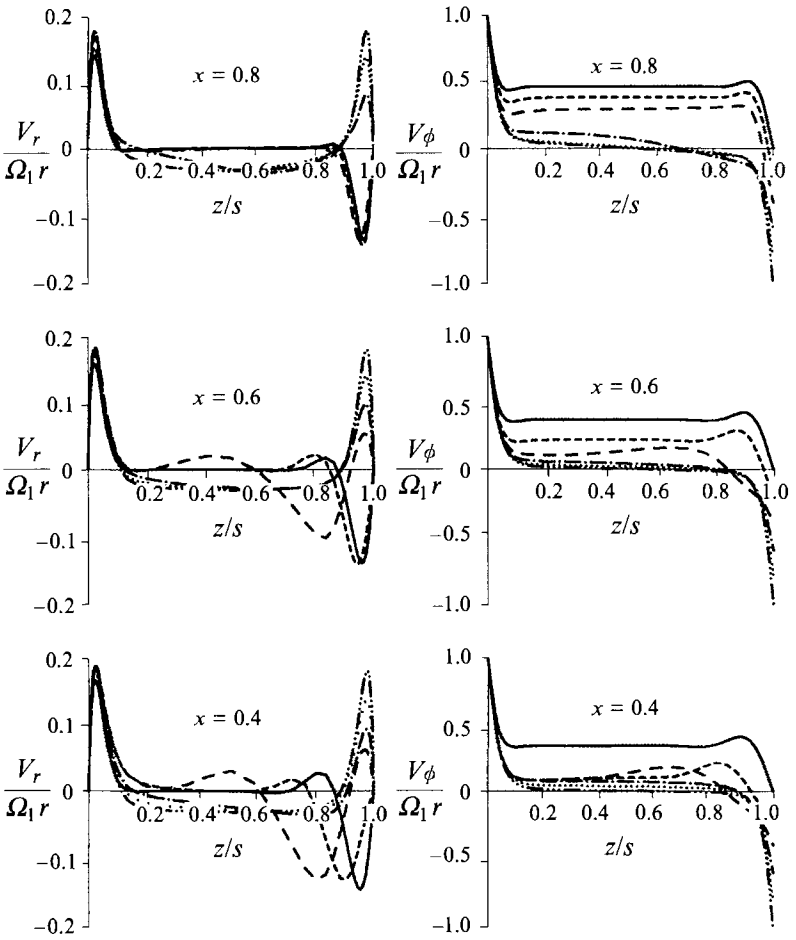

FIGURE 6. Computed turbulent velocity distributions for $Re_\phi = 10^5$, $G = 0.12$. Symbols as for figure 4.

It can also be seen for $x = 0.8$, in figure 6, that when the core rotation is significant (as for $-0.4 \leqslant \Gamma \leqslant 0$), the radial component of velocity in the core is zero. This is consistent with the Taylor–Proudman theorem (see, for example, Batchelor 1967) where, for an inviscid fluid rotating at a constant angular speed, the axial and tangential components of velocity are invariant with z and the radial component is zero. Only when the rotation is zero or very small (as for $-1 \leqslant \Gamma \leqslant -0.6$) does radial inflow occur in the core.

Comparison between the computed and measured velocity profiles is made in §4.

3. Experimental apparatus

Figure 7 shows a schematic diagram of the experimental rig. The disks were 762 mm diameter, disk 1 was made from transparent polycarbonate and disk 2 from steel, and the axial spacing between the disks produced a gap ratio of $G = 0.12$. A polycarbonate shroud was attached to the periphery of each disk, and each shroud and disk assembly could be rotated up to 1500 rev/min in either direction by means of a thyristor-controlled electric motor. The speed was measured, with an uncertainty of ± 1 rev/min, by means of a transducer and timer-counter. The rig was designed to allow a radial

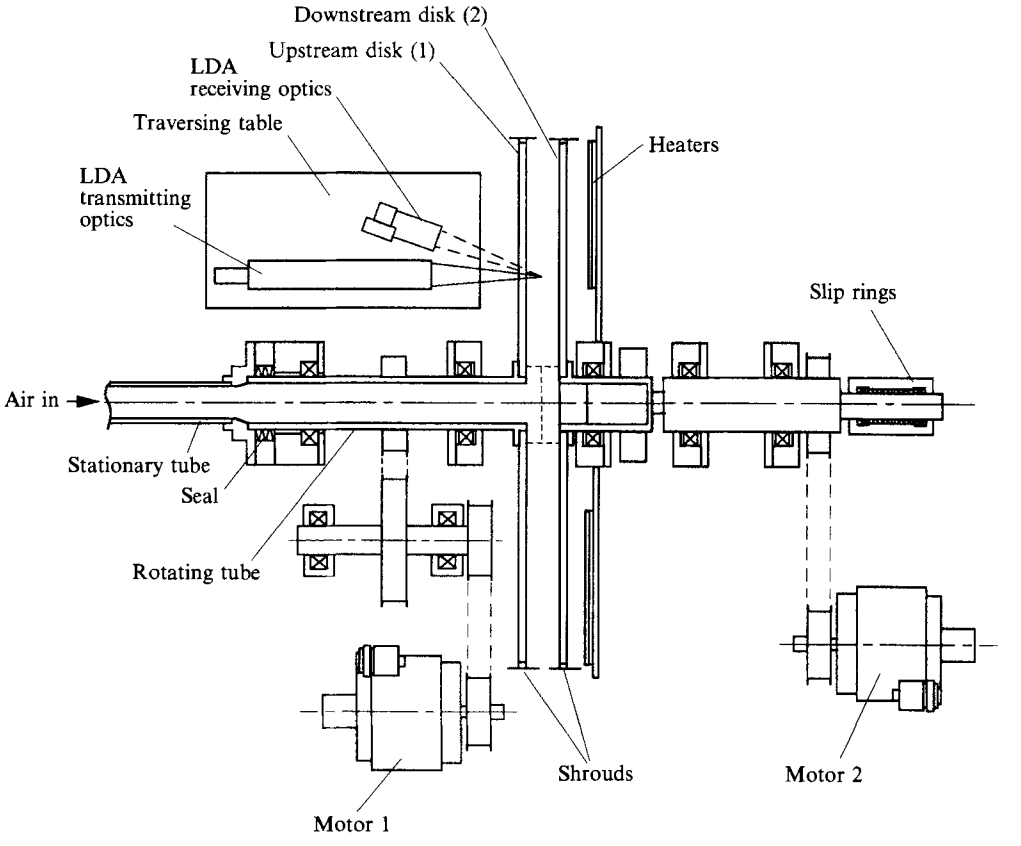

FIGURE 7. Schematic diagram of experimental apparatus.

outflow of cooling air between the disks, and the air could be admitted to the system through two gauze tubes, of 100 mm diameter, each attached to one of the disks: the ratio of the radius of the tube, a, to that of the disks, b, was $a/b = 0.13$.

The radial and tangential components of velocity between the disks were measured at $x = 0.6$, 0.7, 0.8 and 0.85 using a single-component LDA system. The optics were arranged in an off-axis back-scatter mode 'looking through' the polycarbonate disk, as shown in figure 7. The system comprised a 4W Spectra-Physics argon-ion laser together with TSI transmitting optics, frequency shift and receiving optics. The wavelength was 514.5 nm and the power at the 'probe volume' was up to 350 mW. A converging lens of 120 mm focal length and a beam spacing of 50 mm produced a probe volume of 0.34 mm length and 34 μm diameter with a fringe spacing of 1.39 μm.

The Doppler signal was processed using a TSI IFA-750 burst correlator, which could measure frequencies up to 90 MHz with signal-to-noise ratios as low as -5 dB. A Viglen PC was used in conjunction with the processor to control the position of the x–y traversing table on which the optics were mounted. When the signal had been validated by the processor, the PC controlled the movement of the table to its next position. As only one component of velocity could be measured at any one time, it was not possible to measure the turbulence kinetic energy; it was necessary to rotate the transmitting optics manually through 90° to obtain the second component.

The probe volume could be located with a positional uncertainty of 0.13 mm, and it was possible to obtain measurements in the air as close as 0.5 mm from the polycarbonate disk and 1.5 mm from the steel one. It was also possible to make

measurements with the probe volume inside the polycarbonate disk, which produced Doppler signals from 'scattering sites' or impurities within the material. With the disk rotating, the optics were rotated manually until the Doppler frequency was zero: this corresponded to the radial direction, and rotation of the optics through a further 90° corresponded to the tangential direction. Measurements of the disk speed with the LDA system were within 0.5% of those measured by the timer-counter.

The air between the disks was 'seeded' with oil particles of around 1 μm diameter, produced from a Dantec particle generator. The particles were released into the air in the laboratory close to the disks, and sufficient particles were ingested through the clearance between the contra-rotating shrouds to produce acceptable Doppler signals.

4. Comparison between computation and experiment

Before making a comparison between the computations and the measurements obtained from the rig described in §3, the computations were compared with experimental data obtained from a number of sources including the velocity measurements of Itoh, Yamada & Nishioka (1985) for a rotor-stator system and those of Dijkstra & van Heijst (1983) for contra-rotating disks; details are given by Kilic (1993). The agreement was found to be mainly very good, and an example of the comparison with the data of Dijkstra & van Heijst for $\Gamma = -0.3$, $Re_\phi = 2.04 \times 10^4$ and $G = 0.07$ is shown in figure 8.

It should be pointed out that, in the apparatus of Dijkstra & van Heijst, the shroud was attached to disk 1. The velocity of the water between the disks was measured using stereophotography: polystyrene particles were illuminated by flashes of stroboscopic light and the resulting traces were photographed. Knowing the time taken for the particles to move a measured distance enables the speed to be found, and the results ($V_r/\Omega_1 b$ and $V_\phi/\Omega_1 b$) are presented between radial limits of r_{min} and r_{max}, or x_{min} and x_{max} in non-dimensional terms. The current laminar computations, which are presented for the values of x_{min} and x_{max} given for the experiments, are in good agreement with the experimental data and with the computations of Dijkstra & van Heijst; the latter computations are not shown in figure 8. Computations of the value of x_{st}, the non-dimensional radius of the stagnation streamline on the slower disk, were also in good agreement with both the computations and experimental data of Dijkstra & van Heijst.

Figures 9–14 show the comparison between the computations and the velocities measured in the rig described in §3 for $Re_\phi = 10^5$, $G = 0.12$ and $-1 \leqslant \Gamma \leqslant 0$. (For all these figures, the left-hand axes correspond to disk 1, the faster disk.) The non-dimensional velocities, $V_r/\Omega_1 r$ and $V_\phi/\Omega_1 r$, are presented for $0.6 \leqslant x \leqslant 0.85$, which corresponds to the full extent of the experimental range. Computations are shown for both laminar flow and turbulent flow, using the turbulence model of Launder & Sharma (1974) for the latter case.

A value of $Re_\phi = 10^5$ was chosen in an attempt to produce laminar flow. For a free disk (a disk rotating in an infinite quiescent environment), laminar flow becomes unstable at around $x^2 Re_\phi = 2 \times 10^5$ and transition is usually complete around $x^2 Re_\phi = 3 \times 10^5$. For a rotor-stator system transition occurs at lower values of $x^2 Re_\phi$ but $Re_\phi = 10^5$ should ensure that, for $\Gamma = 0$, the flow remains laminar. (It is shown below that whilst the flow does remain laminar for $\Gamma = 0$, turbulent flow can occur at other values of Γ; for all values of Γ, however, the flow in the boundary layer on the faster disk always remains laminar.)

Referring to figure 9 for $\Gamma = 0$, the rotor-stator case, the measurements and

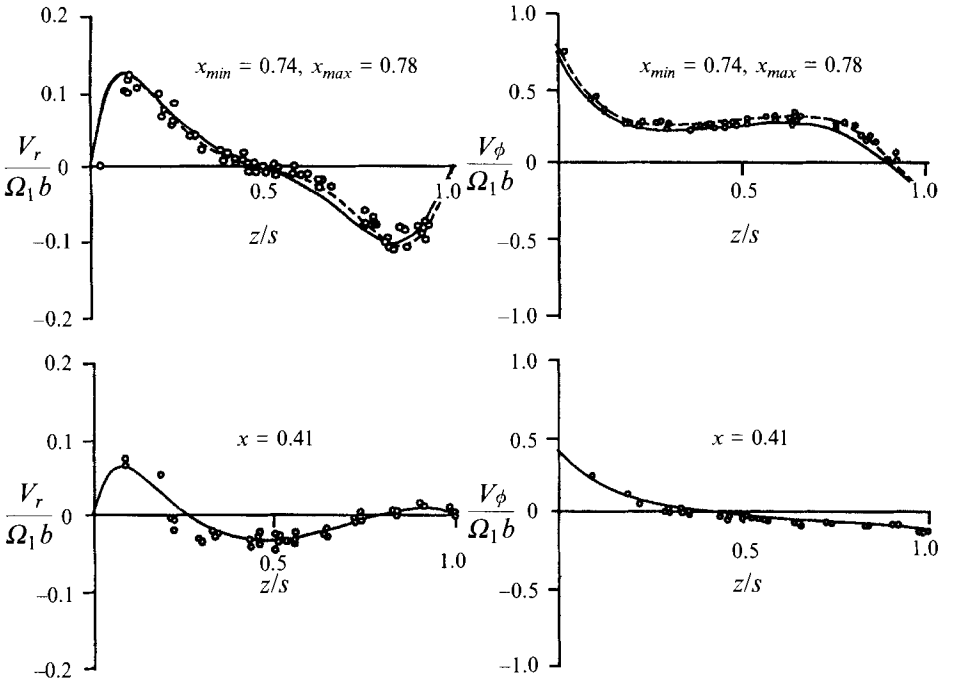

FIGURE 8. Comparisons between laminar computations and experimental data of Dijkstra & van Heijst (1983) for $\Gamma = -0.3$, $Re_\phi = 2.04 \times 10^4$, $G = 0.07$. ---, ——, Computations at higher and lower values of x; ○, measurements.

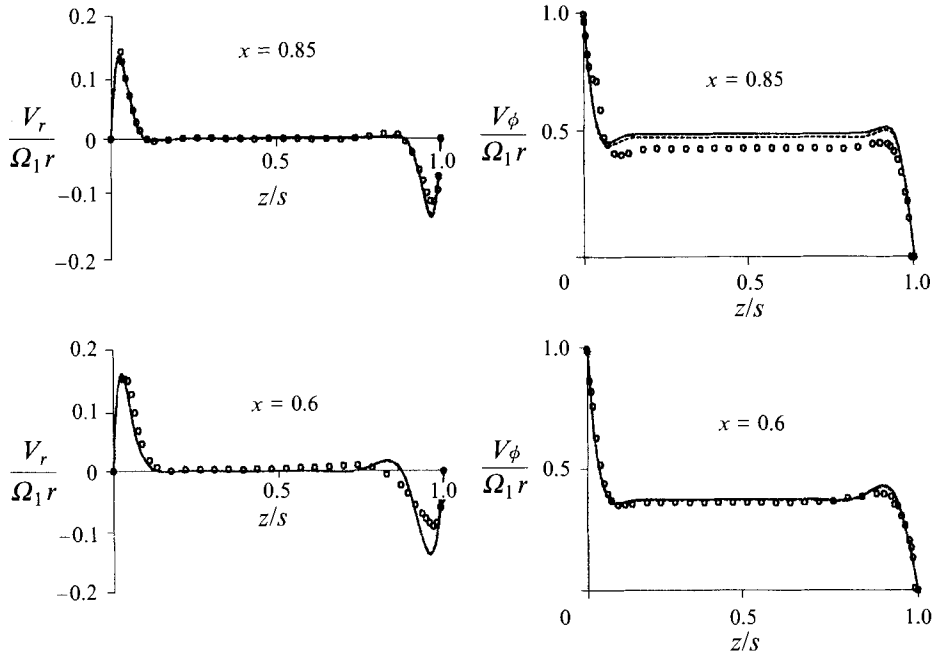

FIGURE 9. Comparisons between computed and measured velocities for $\Gamma = 0$: ——, laminar flow; ——, turbulent flow; ○, measurements.

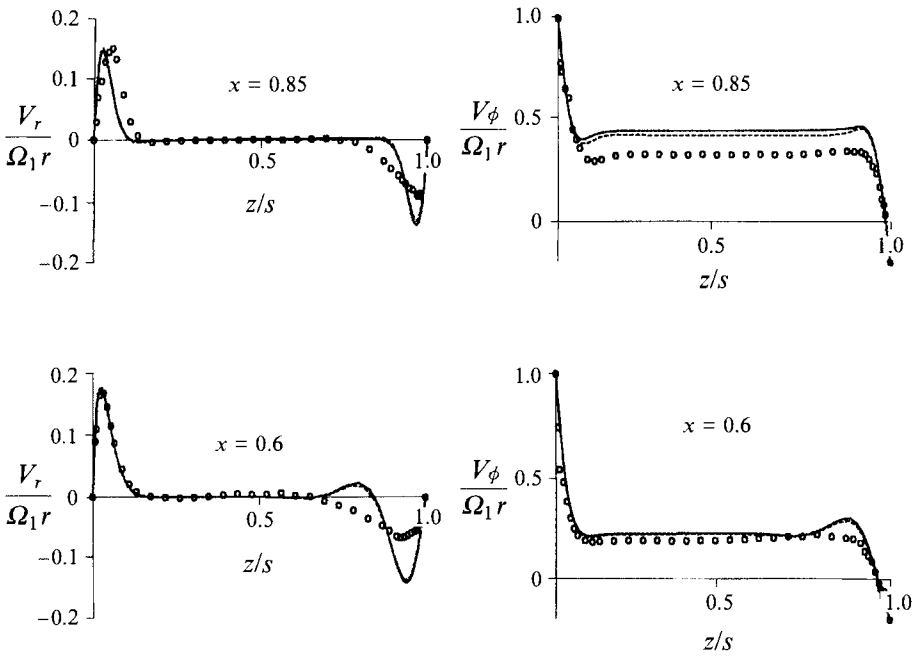

FIGURE 10. As figure 9 but for $\Gamma = -0.2$.

computations show the expected laminar Batchelor-type flow structure. The computed radial components of velocity depart from the measured values near the stator at the smaller value of x, and the computed core rotation is larger than the measured value at the larger value of x; apart from these differences there is very good agreement between the computed and measured velocities. The close agreement between the laminar and turbulent computations shows that there is no tendency for the computed flow to become turbulent, although the thickening of the boundary layer measured on the stationary disk at the smaller radii does suggest that transition may be occurring here.

Figure 10 shows the comparisons for $\Gamma = -0.2$ where again Batchelor-type flow occurs. The agreement between the computations and the measurements is not as good as for the rotor-stator case, particularly near the slower disk for the radial component of velocity and in the core for the tangential component. Again, the similarity between the laminar and turbulent computations suggests that there is no tendency for the computed flow to become turbulent, despite the fact that the measured values of V_r near the slower disk suggest that the radial inflow is turbulent.

The flow structure shows signs of change in figure 11 for $\Gamma = -0.4$. Near the slower disk, both computations and measurements show radial inflow for $x = 0.85$ and outflow for $x = 0.6$ and 0.7; for $x = 0.8$, the computations show inflow and the measurements outflow. These results are consistent with the two-cell structure described above: the experimental measurements suggest a stagnation point on the slower disk for $0.8 < x_{st} < 0.85$, and the computations show $0.7 < x_{st} < 0.8$. The experimental measurements for $x = 0.6$ and 0.7 show that the core rotation is virtually zero and radial inflow occurs over the entire region between the two boundary layers: this is consistent with Stewartson-type flow. The difference between the laminar and turbulent computations at $x = 0.6$, outside the boundary layer on the faster disk, suggests that transition from laminar to turbulent flow is beginning to occur in the

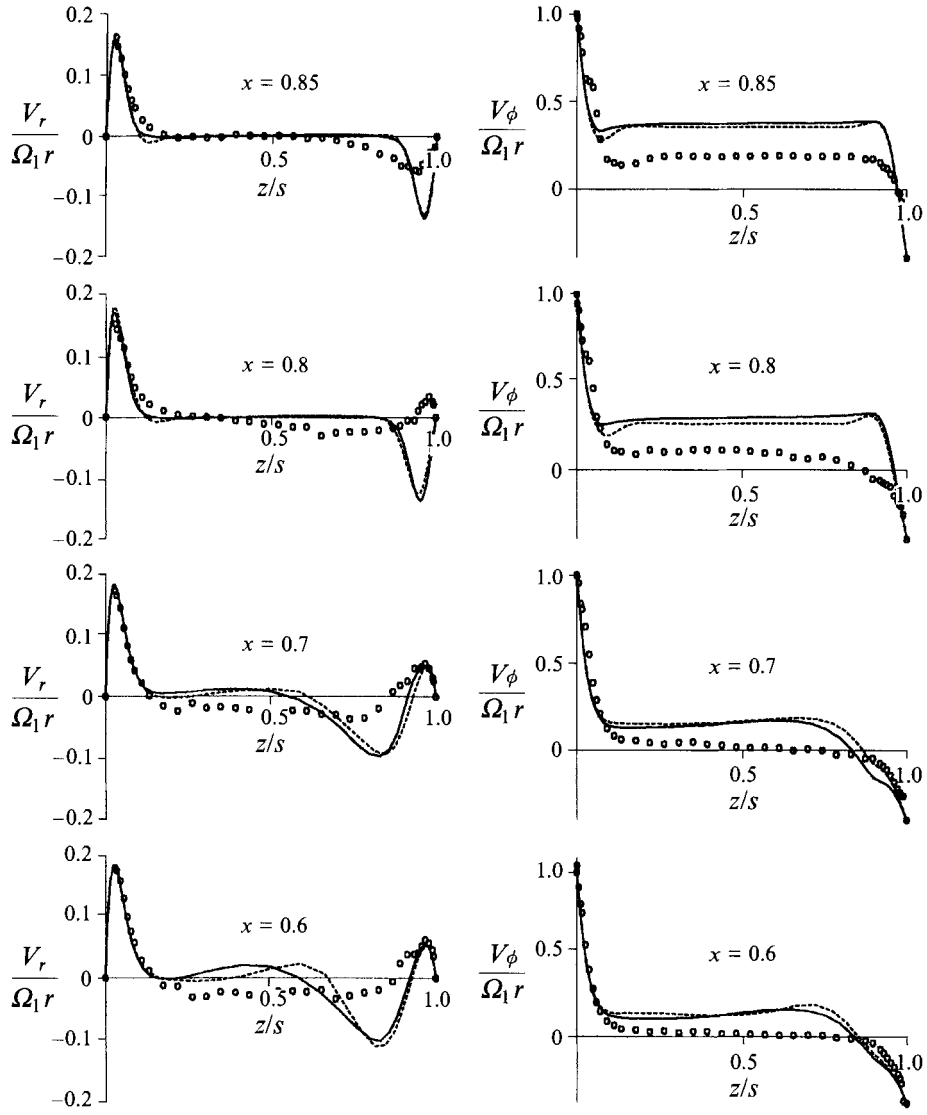

FIGURE 11. As figure 9 but for $\Gamma = -0.4$.

computations; the mainly good agreement between the computations and the measured velocities near the faster disk suggest that the flow remains laminar in this boundary layer. For this value of Γ, there appears to be a double transition: from laminar to turbulent flow and from Batchelor-type flow for $x > x_{st}$ to Stewartson-type flow for $x < x_{st}$.

The results shown in figure 12 for $\Gamma = -0.6$ show further evidence of this double transition. For $x = 0.6$, there is good agreement between the turbulent computations and the measured velocities, both of which show the Stewartson-type flow structure; although not shown here, the agreement for $x = 0.7$ and 0.8 was also good. The laminar computations show a Batchelor-type flow structure, but the large differences between these computations and the turbulent ones indicate that, outside the boundary layer on the faster disk, the flow has become turbulent.

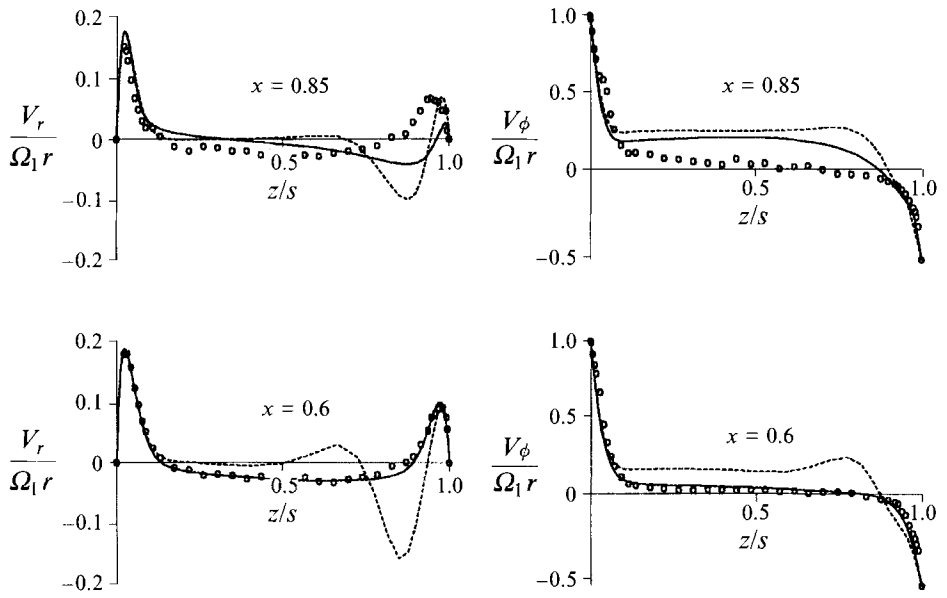

FIGURE 12. As figure 9 but for $\Gamma = -0.6$.

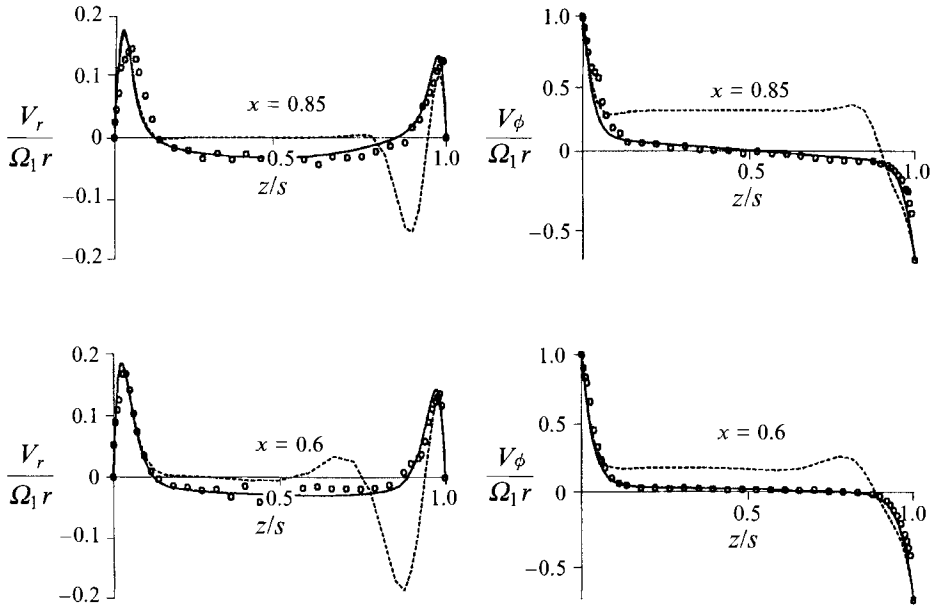

FIGURE 13. As figure 9 but for $\Gamma = -0.8$.

Figures 13 and 14, for $\Gamma = -0.8$ and -1.0 respectively, show mainly good agreement between the turbulent computations and the measurements. Although the laminar computations show Batchelor-type flow, complete with contra-rotating cores of fluid, both the turbulent computations and the measured velocities indicate that Stewartson-type flow occurs.

It is interesting to observe from figure 14 that, for $\Gamma = -1$, the computed laminar and turbulent flow and the measured radial components of velocity are in good agreement in the boundary layers on both disks. This suggests that, although the radial

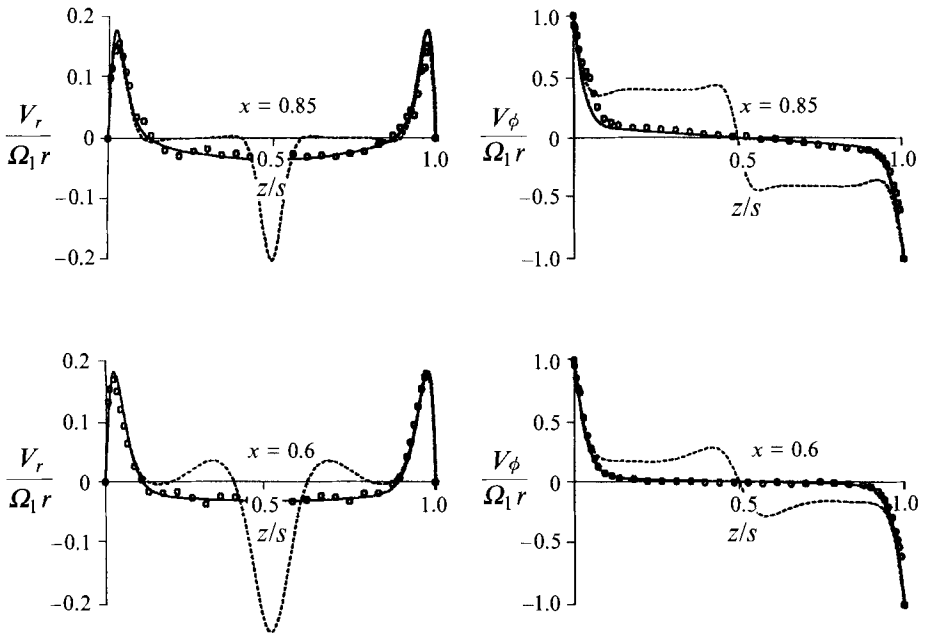

FIGURE 14. As figure 9 but for $\Gamma = -1$.

inflow *outside* the boundary layers is turbulent, the flow *inside* the boundary layers remains laminar. It would appear, therefore, that laminar Batchelor-type flow is basically unstable for $\Gamma = -1$, even for local rotational Reynolds numbers as small as $x^2 Re_\phi = 3.6 \times 10^4$. The computed laminar velocity distributions show points of inflexion in the radial inflow in the mid-plane, and these are associated with instability (see Schlichting 1979). Also, at $r/b = 1$, the contra-rotating axial flows in the boundary layers on the shrouds meet head-on in the mid-plane, creating a large source of turbulence in the radial inflow. Thus, whilst laminar Batchelor-type flow can be computed for $\Gamma = -1$, it does not exist in practice at these rotational Reynolds numbers. Many unsuccessful attempts were made to find experimental evidence of Batchelor-type flow at $\Gamma = -1$, and additional experiments conducted at values of the local rotational Reynolds numbers as low as $x^2 Re_\phi = 2 \times 10^4$ produced no proof of its existence; it was not practicable to conduct experiments at smaller values. Batchelor's (1951) statement that such flows 'may not be realizable experimentally' appears to be true.

With respect to the performance of the Launder–Sharma turbulence model, there is a tendency for it to predict larger regions of laminar flow than have been measured experimentally. This is a common characteristic of low-Reynolds-number k–ϵ turbulence models, and additional computations by Kilic (1993) using Morse's (1988, 1991*a*, *b*) turbulence model showed that there was no significant overall improvement over the Launder–Sharma model. Both models captured the main features of the 'double transition' but neither achieved accurate predictions near the slower disk during the transition process. Iacovides & Toumpanakis (1993) have shown that the incorporation of the so-called Yap correction for the turbulence lengthscale and a rotating-related modification for the dissipation rate can cure some of the problems associated with low-Re k–ϵ models. These modifications have led to improved predictions of the velocity distribution for a rotor-stator system but, as far as the authors are aware, they have not been applied to contra-rotating disks.

5. Conclusions

A combined computational and experimental study has been made of transitional flow between contra-rotating disks in the range $-1 \leqslant \Gamma \leqslant 0$, $0.6 \leqslant x \leqslant 0.85$ and $Re_\phi = 10^5$.

For $Re_\phi = 10^5$ and $\Gamma = 0$, laminar and turbulent computations and experimental measurements show that Batchelor-type flow occurs: there is radial outflow in a boundary layer on the rotating disk, inflow in a boundary layer on the stationary disk, and a rotating core of fluid between the boundary layers. For $\Gamma = -1$, the laminar computations produce Batchelor-type flow: radial outflow occurs in boundary layers on both disks and inflow in a shear layer in the mid-plane, on either side of which is a rotating core of fluid. By contrast, the turbulent computations and the measured velocities for $\Gamma = -1$ show a Stewartson-type flow structure: radial outflow occurs in boundary layers on the disks and inflow occurs throughout the non-rotating core between the boundary layers. It appears that, for $\Gamma = -1$, Batchelor-type flow is unstable: although the radial outflow in the boundary layers on the disks can remain laminar, the inflow creates turbulence and Stewartson-type flow occurs in practice. Laminar computations always produce Batchelor-type flow, but experimental measurements have found no evidence for its existence at $\Gamma = -1$ even at local Reynolds numbers as small as $x^2 Re_\phi = 2 \times 10^4$.

The turbulent computations have shown that, for intermediate values of Γ, transition from Batchelor-type flow to Stewartson-type flow is associated with a two-cell structure, the two cells being separated by a streamline that stagnates at $x = x_{st}$ on the slower disk; Batchelor-type flow occurs for $x > x_{st}$ and Stewartson-type flow for $x < x_{st}$. The measured velocities for $\Gamma = -0.4$ confirm this two-cell structure.

For $Re_\phi = 10^5$, transition from Batchelor-type flow to Stewartson-type flow is associated with transition from laminar to turbulent flow, and consequently the accuracy of the computations depends strongly on the transitional characteristics of the turbulence model used. A common characteristic of low-Re k–ϵ models is to produce unrealistically large regions of laminar flow, and the Launder–Sharma model predicted that the flow would remain laminar in regions where the measurements showed that it was turbulent. This problem is particularly evident for the boundary-layer flow near the slower disk where, for $-0.4 \leqslant \Gamma \leqslant 0$ and $0.6 \leqslant x \leqslant 0.85$, the computations and measurements show laminar and turbulent flow, respectively; as a consequence, the transitional flow structure is poorly predicted for $\Gamma = -0.4$. For all the values of Γ tested, however, the agreement between the computed and measured velocities in the boundary layer on the faster disk is mainly good, and both show the flow to be laminar; for $-1 \leqslant \Gamma \leqslant -0.6$, the agreement between computations and measurements is good over almost the entire region in which measurements were made.

The authors wish to thank the Ministry of Defence and the Science and Engineering Research Council (SERC) for supporting the work described in this paper; in particular, the Meiko parallel computer and much of the TSI LDA system was provided by SERC. We also wish to thank the Turkish Government and the University of Uludag, Bursa, for providing financial support for Dr Kilic.

REFERENCES

BATCHELOR, G. K. 1951 Note on a class of solutions of the Navier–Stokes equations representing steady rotationally-symmetric flow. *Q. J. Mech. Appl. Maths* **4**, 333–354.

BATCHELOR, G. K. 1967 *An Introduction to Fluid Dynamics*. Cambridge University Press.

DIJKSTRA, D. & HEIJST, G. J. F. VAN 1983 The flow between two finite rotating disks enclosed by a cylinder. *J. Fluid Mech.* **128**, 123–154.

DOORMAAL, J. P. VAN & RAITHBY, G. D. 1984 Enhancement of the SIMPLE method for predicting incompressible fluid flows. *Numer. Heat Transfer* **7**, 147–163.

GAN, X., KILIC, M. & OWEN, J. M. 1993 Flow between contra-rotating discs. *ASME Intl Gas Turbine and Aeroengine Congress, Cincinnati*, Paper 93-GT-286. (To appear in *J. Turbomachinery*.)

IACOVIDES, H. & TOUMPANAKIS, P. 1993 Turbulence modelling of flow in axisymmetric rotor-stator systems. *Proc. 5th Intl Symp. on Refined Flow Modelling and Turbulence Measurements, Paris, September, 1993*

ITOH, M., YAMADA, Y. & NISHIOKA, K. 1985 Transition of the flow due to an enclosed rotating disk. *Trans. Japan Soc. Mech. Engrs* **51**, 452–460 (in Japanese).

KARMAN, TH. VON 1921 Über laminare und turbulente reibung. *Z. Angew. Math. Mech.* **1**, 233–252.

KILIC, M. 1993 Flow between contra-rotating discs. PhD thesis, University of Bath, UK.

LAUNDER, B. E. & SHARMA, B. I. 1974 Application of the energy dissipation model of turbulence to the calculation of flow near a spinning disc. *Lett. Heat Mass Transfer* **1**, 131–138.

LONSDALE, G. 1988 Solution of a rotating Navier–Stokes problem by a nonlinear multigrid algorithm, *J. Comput. Phys.* **74**, 177–190.

MORSE, A. P. 1988 Numerical prediction of turbulent flow in rotating cavities. *J. Turbomachinery* **110**, 202–215.

MORSE, A. P. 1991*a* Assessment of laminar-turbulent transition in closed disc geometries. *J. Turbomachinery* **113**, 131–138.

MORSE, A. P. 1991*b* Application of a low Reynolds number k–ϵ turbulence model to high speed rotating cavity flows. *J. Turbomachinery* **113**, 98–105.

PATANKAR, S. V. 1980 *Numerical Heat Transfer and Fluid Flow*. Hemisphere.

SCHLICHTING, H. 1979 *Boundary-Layer Theory*. McGraw Hill.

STEWARTSON, K. 1953 On the flow between two rotating coaxial disks. *Proc. Camb. Phil. Soc.* **49**, 333–341.

VAUGHAN, C. M., GILHAM, S. & CHEW, J. W. 1989 Numerical solutions of rotating disc flows using a non-linear multigrid algorithm. *Proc. 6th Intl Conf. Numer. Meth. Laminar Turbulent Flow, Swansea*, pp. 66–73. Pineridge.

ZANDBERGEN, P. J. & DIJKSTRA, D. 1987 Von Karman swirling flows. *Ann. Rev. Fluid Mech.* **19**, 465–491.